Hindawi Publishing Corporation
International Journal of Photoenergy
Volume 2015, Article ID 893916, 7 pages
http://dx.doi.org/10.1155/2015/893916

Research Article

Investigation of Poly(3,4-ethylenedioxythiophene):Poly(styrenesulfonate) Hole Transport Layer for Solution-Processed Polymer Solar Cells

Chengxi Zhang,[1,2] Jiang Cheng,[1] Xiaoqing Liao,[1] Xiaojuan Lian,[1] Jin Zhang,[1,3] Xin Yang,[1,3] and Lu Li[1]

[1]*Co-Innovation Center for Micro/Nano Optoelectronic Materials and Devices and Research Institute for New Materials Technology, Chongqing University of Arts and Sciences, Chongqing 402160, China*
[2]*College of Materials Science and Engineering, Chongqing University of Technology, Chongqing 400054, China*
[3]*Chongqing Key Laboratory of Environmental Materials and Remediation Technologies, Chongqing University of Arts and Sciences, Chongqing 402160, China*

Correspondence should be addressed to Xin Yang; oyangx2003o@qq.com and Lu Li; lilu25977220@163.com

Received 24 June 2015; Accepted 10 September 2015

Academic Editor: Zhibin Yu

The inverted polymer solar cell was prepared by self-made spray-coating system, and the poly(3,4-ethylenedioxythiophene):poly(styrenesulfonate) (PEDOT:PSS) hole transport layer was studied. 220 nm poly-(3-hexylthiophene):[6,6]-phenylC_{61}butyric-acid methyl-ester (P3HT:PCBM) and 40 nm PEDOT:PSS were deposited on ZnO thin film subsequently by solution spray coating. Different volume of isopropyl alcohol was introduced into PEDOT:PSS to decrease the contact angle and obtain the optimum Marangoni flow. The surface morphology and roughness of PEDOT:PSS films were characterized by atomic force microscopy with varied deposition temperature from 70°C to 160°C. The improvement of power conversion efficiency (PCE) was attributed to the enhancement of vertical phase separation in PEDOT:PSS film, which improved the charge transfer in the bulk cell. The highest PCE of spray-coated PSCs reached 2.80% after postannealing for 10 min.

1. Introduction

Polymer solar cell (PSC) has been intensively investigated over the past decade, due to its superior properties such as mechanical flexibility, light weight, low-cost fabrication, and easily large-area manufacturing compatibility [1–4]. Power conversion efficiency (PCE) surpassing 10% is a milestone of polymer solar cell devices for prospects of commercialization [5, 6]. As a classic PSC polymeric materials, poly-(3-hexylthiophene) (P3HT) and [6, 6]-phenylC_{61}butyric-acid methyl-ester (PCBM) system has shown a praiseworthy potential in increasing PCE. Single-junction bulk-heterojunction (BHJ) solar cells possess interpenetrating networks of electron donor and acceptor, presenting the maximum homogeneous donor/acceptor interfacial area, resulting in more efficient charge separation under illumination. In recent years, the PCE of P3HT:PCBM based PSC has reached 5% [7].

Various approaches have been used to realize an efficient fabrication of the multilayer structure configuration, such as spin coating [8, 9], screen printing [10], ink-jet printing [11], and spray coating [12, 13]. For solution processed method, most of the attention has been captured on spin coating, but it is unsuitable for large-area device or efficient-economical roll-to-roll manufacturing. Spray-coating method can overcome the above drawbacks, which enables uniform thin film and a large-area coating [14].

The inverted PSCs with a configuration of ITO/electron transport layer (ETL)/active layer/hole transport layer (HTL)/metal are widely used. Poly-(3,4-ethylene-dioxythiophene):poly(styrenesulfonate) (PEDOT:PSS) is quite promising as HTL material. The positive effect of PEDOT:PSS

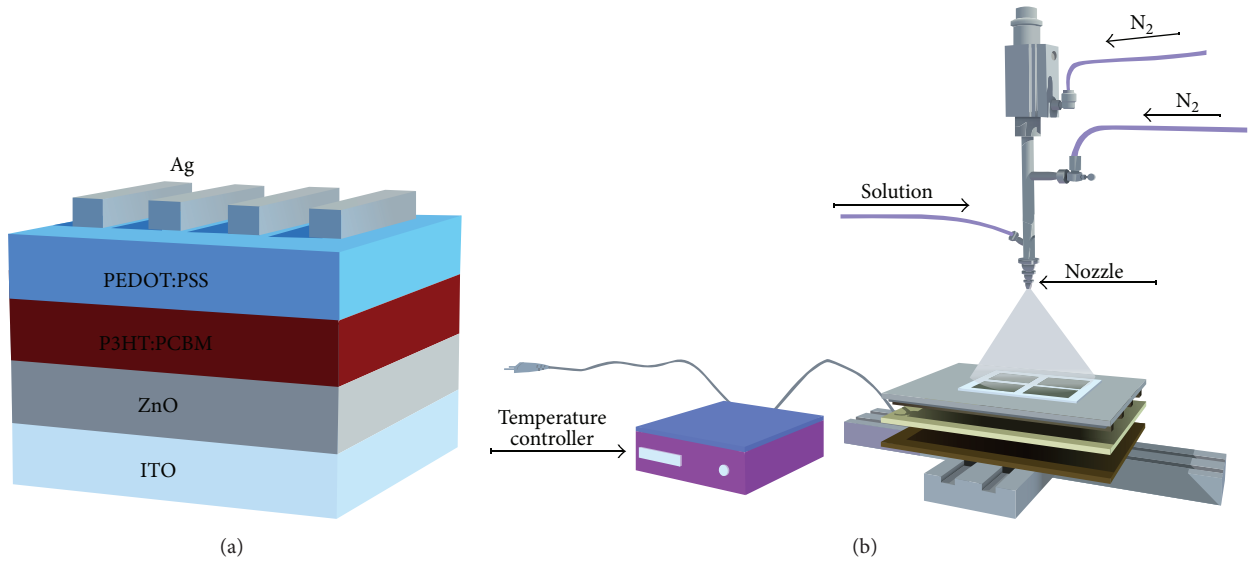

FIGURE 1: The deposition temperature and thickness of each functional layer in PSCs. (a) The typical device architecture of inverted PSC and (b) schematic diagram of spray-coating system.

layer on device performance is attributed to four reasons: improving the selectivity of anode, higher work function than ITO, smooth contact of electrode/active layer, and facilitating the holes transportation [15]. In addition, aqueous precursor of PEDOT:PSS makes it possible to realize all-solution-processed PSC [16]. Although PEDOT:PSS is widely used in inverted PSC, it is still worth noting that PEDOT:PSS layer cannot flat well on P3HT:PCBM, due to the different polarity (PEDOT:PSS is highly hydrophilic and P3HT:PCBM is hydrophobic).

Herein, we reported a facile spray-coating approach to prepare PEDOT:PSS HTL. The surface morphology of PEDOT:PSS film was investigated and prepared by isopropyl alcohol- (IPA-) diluted PEDOT:PSS solution. It was found that the uniformity and roughness of PEDOT:PSS film was affected by the deposition temperature, and the PCE was improved due to the enhancement of vertical phase separation in PEDOT:PSS film. Significantly, after a series of optimizations, the PCE of 2.80% was achieved in this study.

2. Experiment

2.1. Fabrication of PSCs. The device configuration is ITO/ZnO/P3HT:PCBM/PEDOT:PSS/Ag (Figure 1(a)). PSC devices were fabricated on ITO glass substrates (6.7 Ω/sq). The glass was cleaned in ultrasonic bath containing detergent, deionized water, IPA, and acetone (10 min each step) consecutively. Prior to deposition of the ZnO, ITO glass substrates were treated by ultraviolet light for 10 min. Zinc-ammonia precursor was prepared with zinc acetate ($Zn(CH_3COO)_2$, 99.9%, 3 g, Aldrich, USA), and the ZnO layer was sprayed from the zinc-ammonia precursor on ITO glass substrate with a N_2 flow rate of 12 L/min, and then the film was annealed at 200°C for 30 min in air. The photoactive layer precursor that consists of 1 : 1 of P3HT (99.9%, Aldrich) and PCBM (99.9%, Lumtec, USA) was dissolved into 1, 2-dichlorobenzene (DCB) at a concentration of 10 mg/mL and the solution was kept stirring for 12 h at 80°C. The P3HT:PCBM layer was sprayed on the top of ZnO layer at a substrate temperature of 80°C and then annealed at 130°C for 10 min in N_2 atmosphere. PEDOT:PSS dispersion (Heraeus Clevios PH1000) mixed with different volume IPA and 1% Zonyl FS-300 fluorosurfactant was sprayed onto P3HT:PCBM layer at 130°C with a solution injection rate of 0.2 mL/min. The PEDOT:PSS and P3HT:PCBM layers were both deposited with a N_2 flow rate of 10 L/min. Finally, Ag electrode was thermally evaporated in vacuum at 2×10^{-4} Pa through a mask to define five separate cells on each substrate.

2.2. Characterization. The morphology of PEDOT:PSS layer was characterized by atomic force microscope (AFM 5500, Keysight, Inc.) and scanning electron microscope (FEI Quanta 250). The thickness of each layer was monitored using the Alphastep D-100 stylus profiler. The active area of each fabricated PSC was 0.03 cm^2. The photocurrent density-voltage (J-V) curves measurements of PSCs were performed with the xenon lamp (CHF-XM35, Beijing) under a calibrated illumination power of 100 mW/cm^2. All the measurements were carried out in air ambient circumstance.

3. Results and Discussion

3.1. Optimizing of Spray-Coating Parameters. The self-made spray-coating system is shown in Figure 1(b). The nozzle is connected to calibrated syringe pump for solution transporting and N_2-supplier equipment (upper N_2-connector is for pushing up the pin inside and the other is for gas flow controlling). Deposition temperature which plays a crucial role of fabricating HTL is accurately controlled by a thermal couple. The precursor was broken up into small droplets by

Table 1: The deposition temperature and thickness of each functional layer in PSCs.

Layer	Deposition temperature (°C)	Layer thickness (nm)
ZnO	200	50 nm
P3HT:PCBM	40	220 nm
PEDOT:PSS	70, 100, 130, 160	40 nm
Ag	—	120 nm

nozzle and directly sprayed onto temperature controlled ITO substrate.

To form a full wet and continuous PEDOT:PSS layer, the distance between nozzle and substrate was investigated which affected film homogeneity notably. When the height was higher than 8 cm, the small droplets were evaporated completely before reaching hot substrate, thus resulting in a relatively smooth and dry film surface. However, if the height was below 4 cm, the spray-coated PEDOT:PSS film remained wet, resulting in particle aggregation and nonhomogeneous film surface. The best spray distance between nozzle and substrate was 6 cm, at which a continuous and homogeneous film was obtained.

In this work, a computer drove X-Y hotplate stage allows a reproducible thickness of deposited film. The deposition temperature and thickness of each function layer in PSC are summarized in Table 1. By optimizing spray-coating parameters, a better control over the spray-coating processing allowed for improving the performance of PSC.

3.2. Effect of IPA and Fluorosurfactant Doping on PEDOT:PSS Films. During PEDOT:PSS deposition, coffee ring effect and Marangoni flow are paramount factors to determine the morphology of PEDOT:PSS film. The Marangoni flow can be defined as follows: the solute would accumulate at the rim of a drying droplet under the influence of a surface tension gradient. The Marangoni velocity was given by

$$V_c^2(x) = \frac{1}{2\mu(x)}\frac{d\gamma}{dx}x(1-x)\left(-A_1\alpha_1 + A_h\alpha_h\right), \quad (1)$$

where μ is viscosity of the film, γ is surface tension, x is volume fraction of low surface tension solvent, A_l and A_h are evaporation velocity, and α_l and α_h are activity coefficient of the low and high surface tension solvent, respectively [17]. IPA is a favorable candidate to dilute PEDOT:PSS dispersion, since it can improve contact properties effectively between PEDOT:PSS and P3HT:PCBM and ensure full coverage of HTL. Moreover, 1% Zonyl FS-300 fluorosurfactant was added to PEDOT:PSS solution to further reduce the contact angle and enhance spreading on the hydrophobic P3HT:PCBM layer.

It was found that volume ratio of PEDOT:PSS and IPA was 1 : 14 and could not only reduce the contact angle of solution but also control Marangoni flow and convective flows during deposition process, obtaining a relatively homogeneous film. Besides, Girotto et al. [12] elaborated the relationship between contact angle and surface tension, which proved that the diluted PEDOT:PSS solution was beneficial to produce a homogeneous film.

The surface morphologies of PEDOT:PSS films are shown in Figure 2. The original PEDOT:PSS dispersion could not flat well onto P3HT:PCBM layer (Figure 2(a)); however, films prepared with the IPA-diluted solution exhibited a distinguish surface morphology. A network surface was formed (Figure 2(b)), due to the well-flatten droplets on the P3HT:PCBM layer. The network surface could benefit exciton separation at P3HT:PCBM and PEDOT:PSS interface and facilitate charge carrier transporting efficiently to the electrodes. The contact angle was decreased during the preparation of diluted PEDOT:PSS layer and the Marangoni flow was under control. When prepared by adding 1% Zonyl FS-300 fluorosurfactant, PEDOT:PSS film surface was smooth (Figure 2(c)). However, the network structure may provide better pathway for charge carrier transferring than smooth surface, thus resulting in the higher conductivity than that of the other two samples.

In practice, the conductivity of PEDOT:PSS film was also modified with IPA and fluorosurfactant (as shown in Figure 3). With IPA-diluted ratio increasing from 1 : 6 to 1 : 18, the PEDOT:PSS films conductivities were improved from 4.5×10^{-3} S/cm to 1.8×10^{-2} S/cm. However, the films conductivities were decreased to 1.2×10^{-2} S/cm and 3.1×10^{-3} S/cm, respectively, with adding 0.5% and 1% Zonyl FS-300 into PEDOT:PSS solution ((PEDOT:PSS) : IPA = 1 : 14), due to the fact that Zonyl FS-300 fluorosurfactant cannot conduct electricity. Despite this, fluorosurfactant could improve solution ductility and well reduce the contact angle, leading to the well contact between HTL and ETL and the improvement of PCE.

3.3. Effect of Deposition Temperature on the Performance of PSCs. PEDOT:PSS HTL surface topography was significantly influenced by droplets drying rate. Actually, real drying condition of sprayed droplets is a result of extremely complex situation. To estimate the relationship between deposition temperature and drying rate, the average drying rate (dW/dt) (dimensions mass/time) is expressed as follows [18]:

$$\frac{dW}{dt} = \frac{2\pi K_d D_{\text{av}} \Delta T}{\lambda}, \quad (2)$$

where K_d is thermal conductivity of liquid droplet, D_{av} is average droplet diameter, ΔT is mean temperature difference between droplet surface and surrounding air, and λ is latent heat of vaporization. K_d, D_{av}, and λ can be considered as fixed parameters due to the usage of same solution (in this part, the IPA-diluted solution (PEDOT:PSS) : IPA = 1 : 14 and 1% Zonyl FS-300 fluorosurfactant were utilized); thus, the drying rates are dominantly related to ΔT. Therefore, we can assume that the film surface morphology is dominantly related to deposition temperature.

To further control PEDOT:PSS HTL morphology and solution evaporation process, the temperature effect on film surface morphology was also investigated from 70°C to 160°C. Figure 4 show AFM images and vertical phase separation models of PEDOT:PSS films prepared under varied

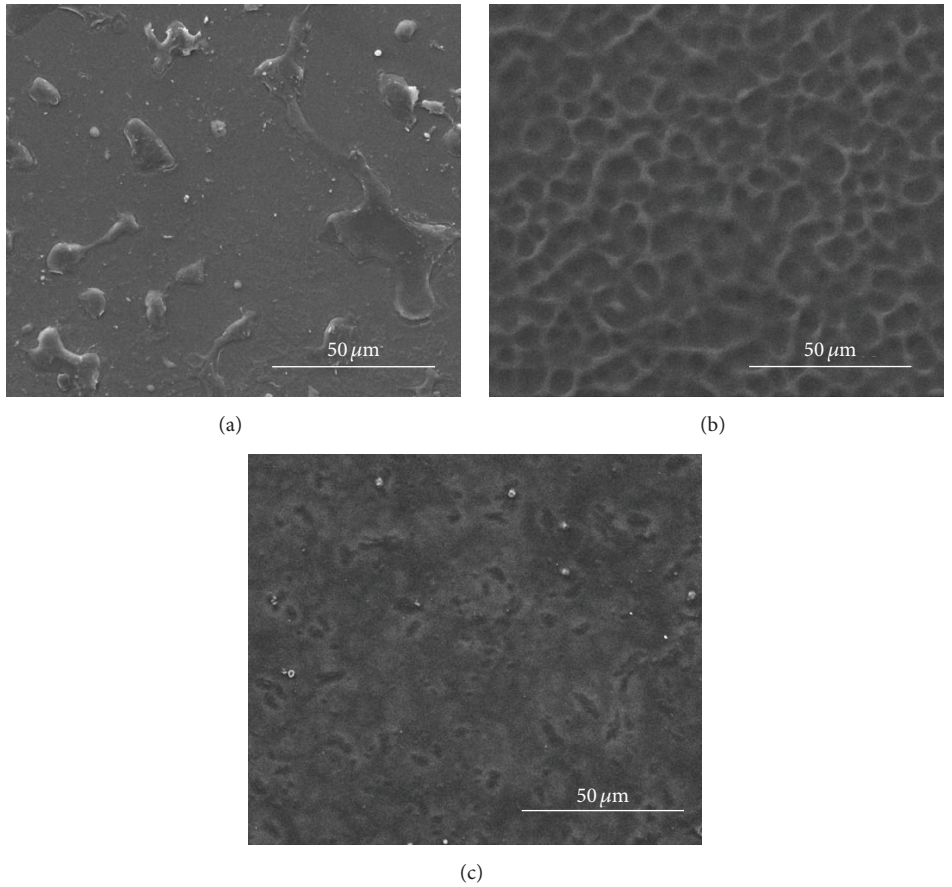

Figure 2: SEM images of PEDOT:PSS film: (a) original PEDOT:PSS dispersion, (b) IPA-diluted solution ((PEDOT:PSS) : IPA = 1 : 14), and (c) IPA-diluted solution ((PEDOT:PSS) : IPA = 1 : 14) doped with 1% Zonyl FS-300 fluorosurfactant. All PEDOT:PSS films were deposited under the same temperature at 130°C with a N_2 flow rate of 10 L/min.

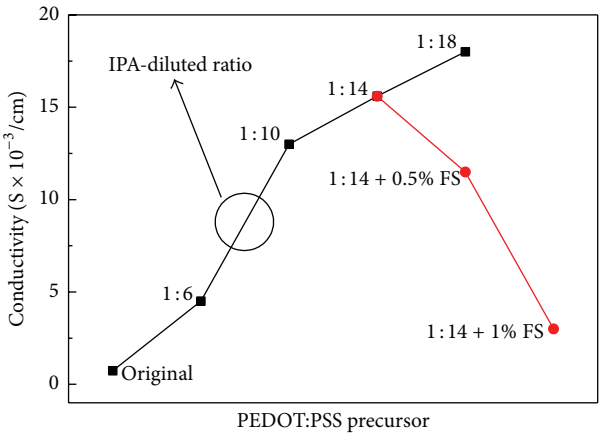

Figure 3: Conductivities of PEDOT:PSS films which are made up of different contents.

deposition temperatures. The different root mean square (RMS) roughness suggested a variation in surface morphology for PEDOT:PSS films. At 70°C, PEDOT:PSS film exhibited the minimum surface roughness with a RMS of 1.0 nm and less phase separation of PEDOT:PSS [16] (Figure 4(a)). When the deposition temperature improved to 100°C, the PEDOT:PSS film exhibited rougher surface with a RMS of 2.0 nm (Figure 4(b)). Further increasing deposition temperature to 130°C, inner PSS moved to film surface and gathered together, giving rise to vertical phase separation effect and forming larger grains (Figure 5(c)). During this process, the contact area between P3HT:PCBM and PEDOT:PSS film interface was enlarged, increasing the possibility of holes in P3HT:PCBM transporting to PEDOT:PSS. Hence, the carriers could be transported through the conductive pathway rather than being recombined with each other in P3HT:PCBM or trapped in PEDOT:PSS HTL [19, 20]. At 160°C, PEDOT:PSS/IPA solution could not wet onto whole P3HT:PCBM layer surface completely due to the escalation of solution evaporation rate. As shown in Figure 4(d), a largest film surface RMS of 7.0 nm was obtained because of the larger grain size caused by high deposition temperature. At this temperature, PSS was completely separated from PEDOT section, leading to the destruction of holes transportation (Figure 5(d)). Furthermore, quite a few defects in PEDOT:PSS/P3HT:PCBM interface caused by rough HTL film could deteriorate device FF and limit the PCE.

The *J*-*V* curves of PSCs for PEDOT:PSS deposited with different temperatures are shown in Figure 6 and the detailed

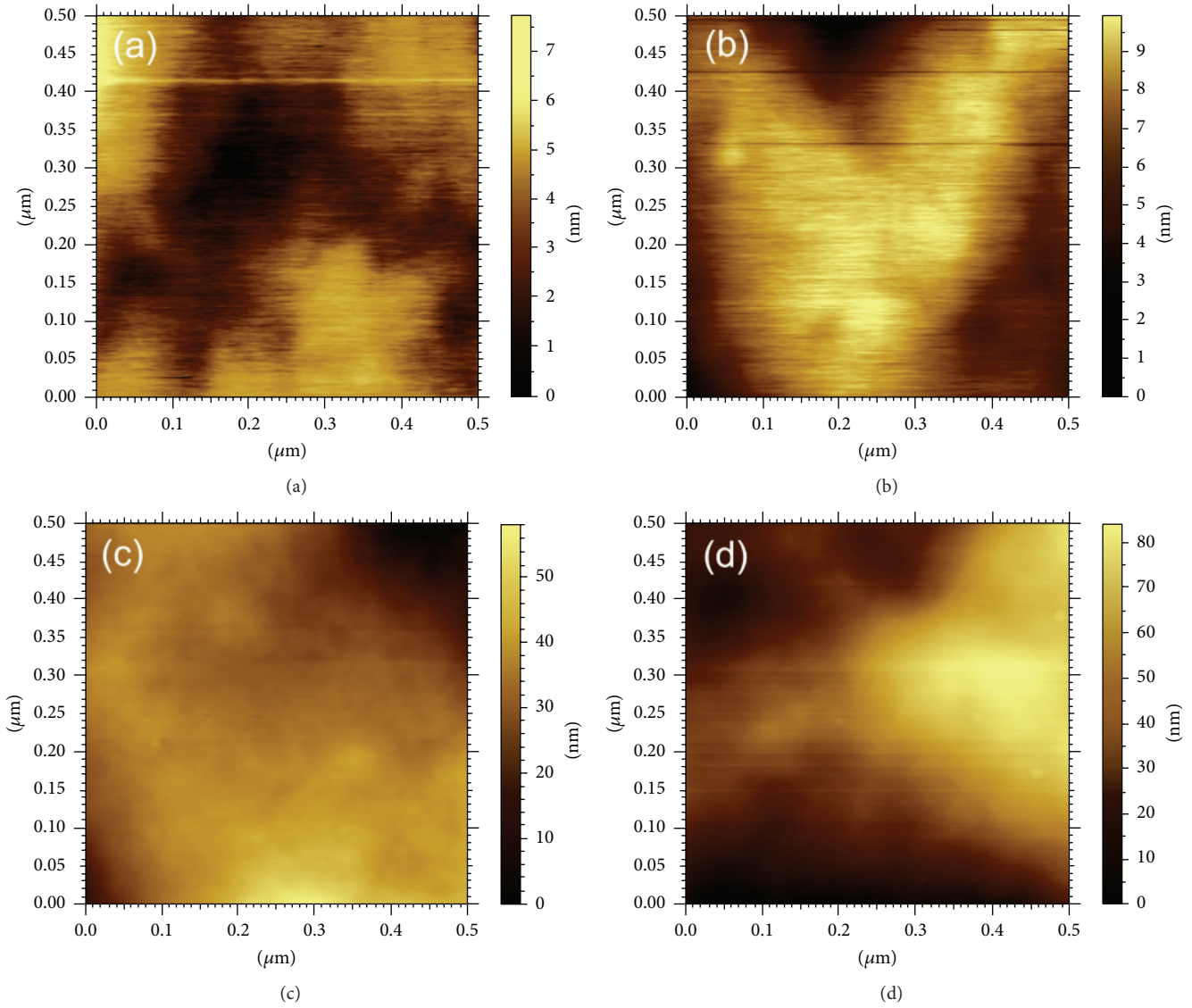

Figure 4: AFM images of PEDOT:PSS films sprayed with different deposition temperatures: (a) 70°C, (b) 100°C, (c) 130°C, and (d) 160°C. The PEDOT:PSS films were deposited with IPA-diluted solution ((PEDOT:PSS) : IPA = 1 : 14) and 1% Zonyl FS-300 fluorosurfactant.

photovoltaic parameters are listed in Table 2. With temperature increasing from 70°C to 130°C, J_{sc} was improved by 30% from 7.05 to 9.17 mA/cm^2 and FF was enhanced from 39.4% to 49.1%, and this rising trend in J_{sc} and FF made a contribution to PCE improvement, from 1.57% to 2.55%. The J_{sc} enhancement could be ascribed to the formation of vertical phase separation between PSS and PEDOT chains which benefited hole transferring from P3HT:PCBM to HTL. Meanwhile, Yeo et al. [21] reported that vertical phase separation in PEDOT:PSS film could increase conductivity and work function of the anode. However, the PCE decreased to 1.40% when deposition temperature was 160°C. On one hand, rougher PEDOT:PSS HTL (as shown in Figure 4(d)) could introduce quite a few defects which might trap hole during the transferring process. On the other hand, the larger PEDOT-rich grains formed by high deposition temperature were completely separated from PSS, deteriorating the conductive pathway for holes migrating and leading to a decrease of J_{sc} and FF. As a result, the optimal deposition temperature to spray PEDOT:PSS solution was 130°C.

Table 2: Performances of PSCs deposited under different temperatures: (a) 70°C, (b) 100°C, (c) 130°C, and (d) 160°C. The PEDOT:PSS films were deposited with IPA-diluted solution ((PEDOT:PSS) : IPA = 1 : 14) and 1% Zonyl FS-300 fluorosurfactant.

TEM (°C)	V_{oc} (V)	J_{sc} (mA/cm^2)	FF (%)	η (%)
70	0.55	7.05	39.4	1.57
100	0.56	7.80	47.0	2.01
130	0.60	9.17	49.1	2.55
160	0.55	7.45	34.7	1.40

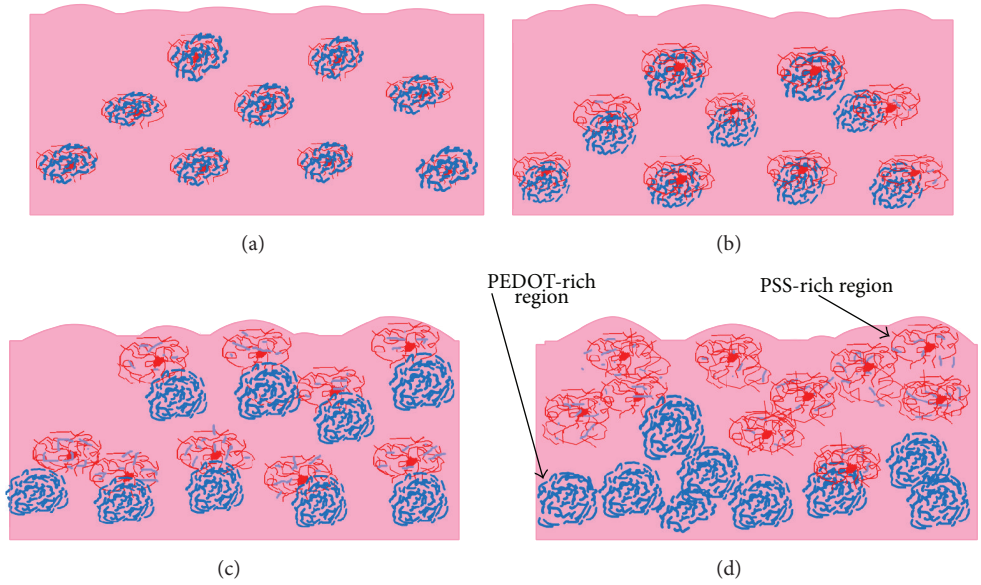

Figure 5: The schematic models of vertical phase separation with different deposition temperatures: (a) 70°C, (b) 100°C, (c) 130°C, and (d) 160°C.

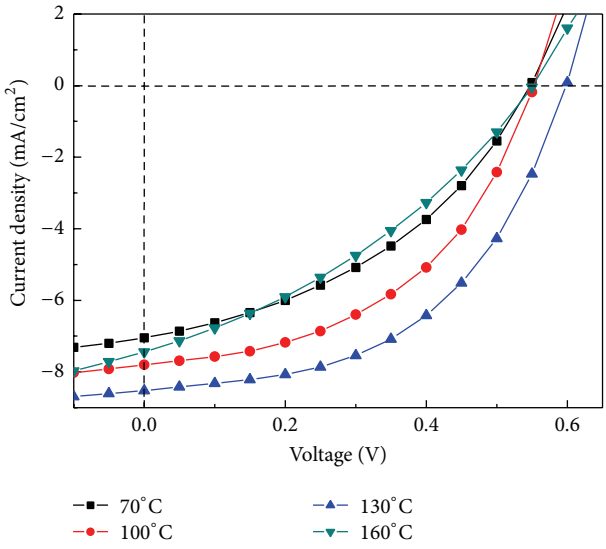

Figure 6: J-V curves of PSCs with PEDOT:PSS deposited under different temperatures: (a) 70°C, (b) 100°C, (c) 130°C, and (d) 160°C. The PEDOT:PSS films were deposited with IPA-diluted solution ((PEDOT:PSS) : IPA = 1 : 14) and 1% Zonyl FS-300 fluorosurfactant.

To further improve interface contact area between PEDOT:PSS and P3HT:PCBM, devices were postannealed on hot plate for 10 min. After that, the best performance of PSC device was 2.80%, which demonstrated a close similar performance to that of spin-coating device [22].

4. Conclusions

In this experiment, a simple spray-coating process for PEDOT:PSS HTL deposition was demonstrated. In order to take advantage of Marangoni flows to control HTL morphology, IPA and fluorosurfactant were used to tune PEDOT:PSS dispersion. The best conductivity was 1.56×10^{-2} S/cm when PEDOT:PSS/IPA ratio was 1 : 14. The vertical phase separation and roughness of HTL were further tuned by varied deposition temperatures. The carriers could transfer through the HTL rather than being recombined with each other in P3HT:PCBM or trapped in HTL. It was found that the vertical phase separation was reinforced with deposition temperature increasing from 70°C to 130°C. Moreover, PSCs were allowed to post-anneal for another 10 min to further improve PCE. After a series of optimizations, the highest PCE of 2.80% was achieved.

Conflict of Interests

The authors declare that there is no conflict of interests regarding the publication of this paper.

Acknowledgments

This research is supported by Chongqing Science and Technology Commission (Grant no. cstc2013 jcyjys50001), Chongqing Education Committee (Grant no. KJ1401113), and Science Projects of Chongqing University of Arts and Sciences (R2013CJ08, Y2013CJ29, XSKY2015123, M2014 ME05).

References

[1] Z. He, C. Zhong, S. Su, M. Xu, H. Wu, and Y. Cao, "Enhanced power-conversion efficiency in polymer solar cells using an inverted device structure," *Nature Photonics*, vol. 6, no. 9, pp. 591–595, 2012.

[2] H.-L. Yip and A. K.-Y. Jen, "Recent advances in solution-processed interfacial materials for efficient and stable polymer

solar cells," *Energy & Environmental Science*, vol. 5, no. 3, pp. 5994–6011, 2012.

[3] G. Li, R. Zhu, and Y. Yang, "Polymer solar cells," *Nature Photonics*, vol. 6, no. 3, pp. 153–161, 2012.

[4] S. H. Park, A. Roy, S. Beaupré et al., "Bulk heterojunction solar cells with internal quantum efficiency approaching 100%," *Nature Photonics*, vol. 3, no. 5, pp. 297–303, 2009.

[5] J. You, L. Dou, K. Yoshimura et al., "A polymer tandem solar cell with 10.6% power conversion efficiency," *Nature Communications*, vol. 4, article 1446, 2013.

[6] M. A. Green, K. Emery, Y. Hishikawa, W. Warta, and E. D. Dunlop, "Solar cell efficiency tables (Version 45)," *Progress in Photovoltaics: Research and Applications*, vol. 23, no. 1, pp. 1–9, 2015.

[7] W. Ma, C. Yang, X. Gong, K. Lee, and A. J. Heeger, "Thermally stable, efficient polymer solar cells with nanoscale control of the interpenetrating network morphology," *Advanced Functional Materials*, vol. 15, no. 10, pp. 1617–1622, 2005.

[8] S.-H. Chan, Y.-S. Hsiao, L.-I. Hung et al., "Morphology evolution of spin-coated films of poly(thiophene-phenylene-thiophene) and [6,6]-phenyl-C_{71}-butyric acid methyl ester by solvent effect," *Macromolecules*, vol. 43, no. 7, pp. 3399–3405, 2010.

[9] J. A. Mikroyannidis, A. N. Kabanakis, S. S. Sharma, and G. D. Sharma, "A simple and effective modification of PCBM for use as an electron acceptor in efficient bulk heterojunction solar cells," *Advanced Functional Materials*, vol. 21, no. 4, pp. 746–755, 2011.

[10] H.-Y. Chen, J. Hou, S. Zhang et al., "Polymer solar cells with enhanced open-circuit voltage and efficiency," *Nature Photonics*, vol. 3, no. 11, pp. 649–653, 2009.

[11] S. H. Eom, H. Park, S. H. Mujawar et al., "High efficiency polymer solar cells via sequential inkjet-printing of PEDOT:PSS and P3HT:PCBM inks with additives," *Organic Electronics*, vol. 11, no. 9, pp. 1516–1522, 2010.

[12] C. Girotto, D. Moia, B. P. Rand, and P. Heremans, "High-performance organic solar cells with spray-coated hole-transport and active layers," *Advanced Functional Materials*, vol. 21, no. 1, pp. 64–72, 2011.

[13] L.-M. Chen, Z. Hong, W. L. Kwan et al., "Multi-source/component spray coating for polymer solar cells," *ACS Nano*, vol. 4, no. 8, pp. 4744–4752, 2010.

[14] C. Girotto, B. P. Rand, J. Genoe, and P. Heremans, "Exploring spray coating as a deposition technique for the fabrication of solution-processed solar cells," *Solar Energy Materials and Solar Cells*, vol. 93, no. 4, pp. 454–458, 2009.

[15] Z. Hu, J. Zhang, Z. Hao, and Y. Zhao, "Influence of doped PEDOT:PSS on the performance of polymer solar cells," *Solar Energy Materials and Solar Cells*, vol. 95, no. 10, pp. 2763–2767, 2011.

[16] Y. Zheng, S. Li, X. Yu, D. Zheng, and J. Yu, "Investigation of in situ annealing on poly(3,4-ethylenedioxythiophene):poly(styrenesulfonate): towards all-solution-processed inverted polymer solar cells," *RSC Advances*, vol. 4, no. 32, pp. 16464–16471, 2014.

[17] Y. Zheng, S. Li, W. Shi, and J. Yu, "Prepare dispersed CIS nano-scale particles and spray coating CIS absorber layers using nano-scale precursors," *Nanoscale Research Letters*, vol. 9, article 1, 2014.

[18] B.-K. Yu, D. Vak, J. Jo et al., "Factors to be considered in bulk heterojunction polymer solar cells fabricated by the spray process," *IEEE Journal on Selected Topics in Quantum Electronics*, vol. 16, no. 6, pp. 1838–1846, 2010.

[19] T. M. Clarke and J. R. Durrant, "Charge photogeneration in organic solar cells," *Chemical Reviews*, vol. 110, no. 11, pp. 6736–6767, 2010.

[20] W. Zhang, R. Hu, D. Li, M.-M. Huo, X.-C. Ai, and J.-P. Zhang, "Primary dynamics of exciton and charge photogeneration in solvent vapor annealed P3HT/PCBM films," *The Journal of Physical Chemistry C*, vol. 116, no. 6, pp. 4298–4310, 2012.

[21] J.-S. Yeo, J.-M. Yun, D.-Y. Kim et al., "Significant vertical phase separation in solvent-vapor-annealed poly(3,4-ethylenedioxythiophene):poly(styrene sulfonate) composite films leading to better conductivity and work function for high-performance indium tin oxide-free optoelectronics," *ACS Applied Materials & Interfaces*, vol. 4, no. 5, pp. 2551–2560, 2012.

[22] J.-W. Kang, Y.-J. Kang, S. Jung et al., "Fully spray-coated inverted organic solar cells," *Solar Energy Materials and Solar Cells*, vol. 103, pp. 76–79, 2012.